

A modified first-motion approximation for the synthesis of body-wave seismograms

George R. Mellman and Donald V. Helmberger

Seismological Laboratory California Institute of Technology, Pasadena, California

Received 1977 November 25; in original form 1977 June 24

Summary. Modified first-motion approximations have been developed for the generation of synthetic body-wave seismograms using the Cagniard–de Hoop method. Comparisons are presented between classical first motion, modified first motion and full Cagniard treatments for problems involving a homogeneous sphere and a triplication in a realistic earth model. Results of these comparisons show that the modified first-motion approximations may be used for a wide variety of geophysically interesting problems with little loss of accuracy compared to the full Cagniard method.

Introduction

Body-wave synthetic seismograms have been extensively used in recent years to study a wide variety of earthquake source and earth-structure problems. Two methods have primarily been used for the calculation of synthetic seismograms, the reflectivity method of Fuchs & Müller (1971) and the Cagniard–de Hoop method (de Hoop 1960). The principal drawback of both of these methods is that they require relatively long, expensive computer programs. Recently Wiggins (1976) and Chapman (1976) have independently developed a first-motion method which greatly reduces the computer time needed for the generation of synthetic seismograms, but appears to be somewhat restrictive in application to geophysical problems.

First-motion approximations have been known in geophysics for a number of years (Gilbert & Knopoff 1961). While they provide a great deal of insight, they have until recently proved to be of little use in the calculation of synthetic seismograms. This paper presents a modification of the standard Cagniard–de Hoop first-motion approximation that allows for rapid calculation of synthetic seismograms for a wide variety of problems. This Modified First-Motion method (MFM) retains the advantages of physical insight provided by the Cagniard–de Hoop method, while requiring significantly less computation and hence computer time. In addition, the method is compatible with the standard Cagniard–de Hoop method, so that significant savings may be realized even in cases where MFM is not entirely applicable.

Classical first-motion approximation

We take as our starting point the Cagniard-de Hoop high-frequency approximation for displacement potential of a generalized ray reflected from the n th interface in a layered elastic stack, (Helmberger 1968).

$$\phi(t) = \psi(t) * 1/\sqrt{t} * S'(t) \quad (1)$$

$$\psi(t) = \text{Im} [\sqrt{2p/r} (1/\pi\eta_1) R_n(p) T(p) dp/dt],$$

where $R_n(p)$ is the complex generalized plane-wave reflection coefficient for the $n-1$, n layer interface; $T(p) \equiv \Pi_i T_i(p)$ is a product of plane-wave transmission coefficients, $S'(t)$ is the derivative of the source-time function, r is the range, and p is the ray parameter. The relationship between p and t for a given generalized ray is:

$$t = pr + \sum_{i=1}^{n-1} 2h_i \eta_i, \quad \text{Im}[T(p)] = 0, \quad (2)$$

where h_i is the thickness of the i th layer, c_i is the elastic velocity in the i th layer and $\eta_i = (1/c_i^2 - p^2)^{1/2}$.

The contour defined by equation (2) leaves the real p axis at p_0 such that $dt/dp(p_0) = 0$, corresponding to the ray parameter and arrival time t_0 of the geometric ray. If $p_0 > 1/c_n \equiv p_c$, then the reflection coefficient $R_n(p)$ becomes complex for $p > p_c$ and a head wave is present. In this case the head wave is the first arrival, at a time $t_c < t_0$.

It is convenient, at this point, to restrict our discussion to fluid models, since the expression for $R_n(p)$ is simple in this case. It should be noted however, that the approximations that are developed may be readily applied to solid elastic models as well.

In the classical first-motion approximation, we attempt to approximate ψ by approximating the most rapidly varying quantities in ψ near $p = p_c$ and p_0 , while considering all other quantities to be constant. In the neighbourhood of p_c , the most rapidly varying quantity is η_n . Since, by definition $\eta_n = (p + 1/c_n)^{1/2} (1/c_n - p)^{1/2}$, and in the neighbourhood of p_c , $p - p_c \approx (t - t_c) dp/dt(p_c)$ we have

$$\eta_n \approx i\sqrt{2/c_n} (t - t_c)^{1/2} [dp/dt(p_c)]^{1/2}. \quad (3)$$

For a fluid, we have

$$R_n(p) = \frac{\eta_{n-1} - \delta \eta_n}{\eta_{n-1} + \delta \eta_n} \quad (4)$$

and

$$\text{Im}(R_n) = \frac{2\delta \text{Im} \eta_n \eta_{n-1}}{|\delta \eta_n|^2 + |\eta_{n-1}|^2}, \quad (5)$$

where

$$\delta = \frac{\rho_{n-1}}{\rho_n}.$$

Since $|\eta_n| \ll |\eta_{n-1}|$ in the neighbourhood of t_c we have

$$\text{Im} R_n(t) \approx -2i\delta \frac{\eta_n}{\eta_{n-1}} \quad (6)$$

and

$$\psi(t) \approx \frac{2}{\pi\eta_1} \delta \sqrt{2/c_n} [dp/dt(p_c)]^{3/2} \sqrt{2p_c/r} (t-t_c)^{1/2}. \quad (7)$$

If we now assume a step function source and recognizing that $[dt/dp(p_c)] \equiv L$ is the distance travelled in the refractor, we find

$$\phi(t) = \frac{4\delta}{\eta_1(p_c)} \frac{1}{c_n \sqrt{rL^3}} (t-t_c), \quad t_c < t. \quad (8)$$

Thus, the time dependence of the head wave is the integral of the source-time function.

In the neighbourhood of t_0 , the most rapidly varying quantity is dp/dt . Using a Taylor series for t and keeping only the first non-zero term, we have

$$t-t_0 \approx \frac{1}{2}(p-p_0)^2 \frac{d^2t}{dp^2}(p_0) \quad (9)$$

and solving for $p-p_0$ and differentiating,

$$\frac{dp}{dt} \approx \frac{1}{(t-t_0)^{1/2} (2d^2t/dp^2)^{1/2}} = \frac{1}{(t_0-t)^{1/2} (2|d^2t/dp^2|)^{1/2}}, \quad (10)$$

since $d^2t/dp^2(p_0) < 0$.

This gives us

$$\psi(t) \approx \sqrt{p_0/r} \frac{1}{\pi\eta_1} \text{Im}[R(p_0)] T(p_0) \left| \frac{d^2t}{dp^2} \right|^{-1/2} (t_0-t)^{-1/2}, \quad t < t_0, \quad (11a)$$

$$\psi(t) \approx \sqrt{p_0/r} \frac{1}{\pi\eta_1} \text{Re}[R(p_0)] T(p_0) \left| \frac{d^2t}{dp^2} \right|^{-1/2} (t-t_0)^{-1/2}, \quad t > t_0. \quad (11b)$$

Convolution with $1/\sqrt{t}$ assuming a step-function source gives for (11a)

$$\phi(t) = -\sqrt{p_0/r} \frac{1}{\pi\eta_1(p_0)} \text{Im}[R_n(p_0)] \left| \frac{d^2t}{dp^2} \right|^{-1/2} \ln \left(\frac{|t_0-t|}{2t_0} \right) \quad (12a)$$

and for (11b)

$$\phi(t) = \sqrt{p_0/r} \frac{1}{\eta_1(p_0)} \text{Re}[R_n(p_0)] T(p_0) \left| \frac{d^2t}{dp^2} \right|^{-1/2} H(t-t_0), \quad (12b)$$

where $H(t)$ is the Heaviside function.

The expression (12a) contains the log singularity that characterizes a critical reflection and (12b) is the step response obtained from geometric optics. For $p_0 > 1/c_n$, the total response is given by (12b). Thus, the first-motion approximation always gives the source-time function for pre-critical reflections. Rather abruptly, at ranges where $p_0 > 1/c_n$, there develops an additional critical reflection term, given by (12a) which, due to the singularity at t_0 , dominates the response. For ranges where $p_0 \gg 1/c_n$, the integral of the time function given by (8), becomes the dominant feature.

Some of the problems associated with the standard first-motion approximations may be seen from the profile of generalized rays in Fig. 1. As may be seen from (1a), even pre-critical generalized rays exhibit appreciable differences in shape from the step function predicted by the first-motion approximations. Further problems are present for critical

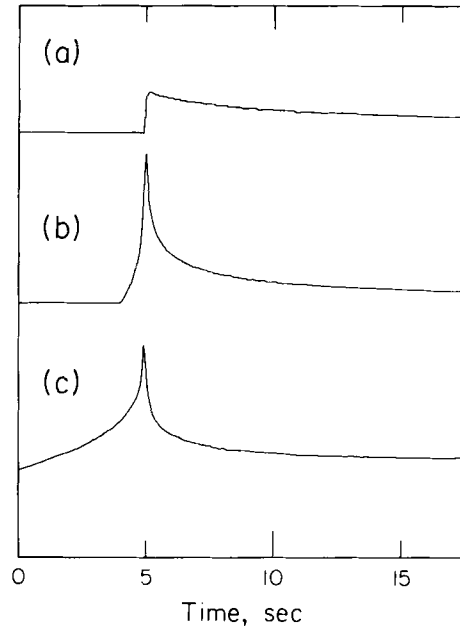


Figure 1. Profile of step-function responses for a fluid interface illustrating typical waveforms for (a) near-vertical reflection, (b) near-critical reflection, (c) well-developed refraction.

reflections where p_0 is near p_c , since there is no mechanism in the first-motion approximations for joining the two approximations used for $t < t_0$. To do this, we must modify the approximations used to obtain a single expression that agrees with the standard expressions for ψ near t_0 and t_c , but is valid for all $t_c < t < t_0$.

The modified first-motion approximations

We wish to find an approximation which will preserve first-motion behaviour of ψ in the neighbourhood of t_0 and t_c and vary continuously in between. In addition, we wish to do this in such a way that little or no information other than that used for the standard first-motion approximations is needed.

It will again be convenient to consider the head-wave and reflected-wave portions of ψ separately. For the head-wave portion, where $t < t_0$, we will modify the standard first-motion approximations for η_n and dp/dt by the addition of higher-order terms that leave the standard approximations unchanged in the neighbourhood of the original expansion point, but also give the correct values of $\eta_n(t_0)$ and $dp/dt(t_c)$. In addition, it will be necessary to develop approximate expressions for η_{n-1} and $T(p)$. All other quantities will be considered to be constant.

We start with the approximate expression for dp/dt given by (10):

$$dp/dt \approx 2 \left(\left| \frac{d^2 t}{dp^2} \right| \right)^{-1/2} (t_0 - t)^{1/2}.$$

We note that addition of terms of the form $a_\alpha (t_0 - t)^m$ where $m \geq 0$ have no effect on the behaviour of dp/dt in the neighbourhood of t_0 . Thus, we may generate the desired approximation by addition of such terms to (10) and appropriate choice of constants. The simplest

such approximation is

$$dp/dt = \left(2 \left| \frac{d^2 t}{dp^2} (p_0) \right| \right)^{-1/2} [(t_0 - t)^{-1/2} + a_\alpha] \quad (13)$$

$$a_\alpha = \frac{dp}{dt} (p_c) \left(2 \left| \frac{d^2 t}{dp^2} (p_0) \right| \right)^{1/2} - (t_0 - t_c)^{-1/2},$$

which also preserves the monotone increasing behaviour of dp/dt .

Similarly, we may modify equation (3),

$$\eta_n \approx i [2/c_n dp/dt(p_c)]^{1/2} (t - t_c)^{1/2}$$

by the addition of terms of the form $a_n(t - t_c)^m$, $m \geq 1$, without changing the behaviour of η_n in the neighbourhood of p_c . Thus we have

$$\eta_n \approx i [2/c_n dp/dt(p_c)]^{1/2} (t - t_c)^{1/2} [1 + (t - t_c) a_n] \quad (14)$$

$$a_n = \{\eta_n(p_0) [2/c_n dp/dt(p_c)]^{-1/2} (t_0 - t_c)^{-1/2} - 1\} / (t_0 - t_c)$$

which preserves the behaviour of $\eta_n(p, c)$, as well as the value of $\eta_n(p, 0)$.

In order to approximate $\text{Im}(R_n)$ accurately over the entire range $t_c < t < t_0$, it is necessary to have an approximation for η_{n-1} , as well as η_n . One method of obtaining such an approximation is to integrate the approximation for dp/dt given in (13) to obtain an explicit expression for p in terms of t . We may then substitute this expression into the expression for η_{n-1} to obtain an explicit expression for η_{n-1} in terms of t . As this expression is somewhat cumbersome however, we use a further approximation of this expression, namely

$$\eta_{n-1} \approx a_p(t_p - t)^{1/2}, \quad (15)$$

where a_p and t_p are chosen such that the values of $\eta_{n-1}(t_c)$ and $\eta_{n-1}(t_0)$ are preserved.

For $t_c < t < t_0$, we have from (1) and (5)

$$\psi = \frac{1}{\pi \eta_1} \sqrt{p/r} T(p) \frac{2 \delta \text{Im} \eta_{n-1} \eta_n}{|\eta_{n-1}|^2 + \delta^2 |\eta_n|^2} dp/dt. \quad (16)$$

Replacing dp/dt , η_n and η_{n-1} with their approximate time-domain expressions and replacing all other terms by their values at p_0 , we obtain an explicit time-domain expression for ψ .

If $p_0 \approx 1/c_{n-1}$, then the assumption that $T(p)$ is constant is violated. In this case, using $T(p_0)$ gives much too small a value for the head wave. Instead, we use a value of p where $\text{Im}[R_n(p)]$ has a maximum, since this is the region from which the greatest contribution to the head wave will arise. Thus, we evaluate $T(p)$ at $p = \min [p_0, \sqrt{(1/c_{n-1}^2 + \delta^2/c_n^2)/(1 + \delta^2)}]$ and then make the assumption that $T(p)$ is constant.

If $(t_0 - t_c)$ is not large compared to the time-point spacing, then the expressions that we have developed will fail to give a good approximation of ψ . In this case, the area under ψ , rather than the actual shape of ψ , is important. We may thus determine

$$\int_{t_c}^{t_0} \psi dt,$$

and replace ψ with a convenient functional form having the appropriate area. For simplicity a triangle may be used, starting at t_c and having its maximum at t_0 . To determine the area,

we note that

$$\begin{aligned} I &\equiv \int_{t_c}^{t_0} \psi dt = \int_{t_c}^{t_0} \frac{1}{\pi \eta_1} \sqrt{2p/r} T(p) \frac{2\delta \eta_{n-1} \operatorname{Im} \eta_n}{|\eta_{n-1}|^2 + \delta^2 |\eta_n|^2} (dp/dt) dt \\ &= \int_{p_c}^{p_0} \frac{1}{\pi \eta_1} \sqrt{2p/r} T(p) \frac{2\delta \eta_{n-1} \operatorname{Im} \eta_n}{|\eta_{n-1}|^2 + |\delta \eta_n|^2} dp. \end{aligned}$$

Making the approximation that $\eta_i \approx \sqrt{2/c_i} (1/c_i - p)^{1/2}$, we have

$$\begin{aligned} I &\approx \frac{4\delta}{\pi \eta_1(p_0)} \sqrt{2p_0/r} T(p_0) \frac{1}{\sqrt{c_n c_{n-1}}} \int_{p_c}^{p_0} (p - 1/c_n)^{1/2} (1/c_{n-1} - p)^{1/2} dp \\ &= \frac{4\delta}{\pi \eta_1(p_0)} \sqrt{2p_0/r} T(p_0) \frac{1}{\sqrt{c_n c_{n-1}}} \left[(1/4) (2p_0 - 1/c_{n-1} - p_c) \sqrt{(1/c_1 - p_0)(p_0 - p_c)} \right. \\ &\quad \left. + (\pi/16) (1/c_{n-1} - p_c)^2 - (1/8) (1/c_{n-1} - p_c)^2 \sin^{-1} \left(\frac{(1/c_{n-1} + p_c - 2p_0)}{1/c_{n-1} - p_c} \right) \right]. \end{aligned} \quad (17)$$

For $t > t_0$, we retain the first-motion approximation (10) for dp/dt . We do not however, maintain the assumption that R_n is constant. Instead, we use the approximate contour, given by

$$t - t_0 \approx (1/2) (p - p_0)^2 \frac{d^2 t}{dp^2} + (1/6) (p - p_0)^3 \frac{d^3 t}{dp^3}. \quad (18)$$

Using the second term on the right-hand side of (18) as a perturbation, we obtain

$$\begin{aligned} p - p_0 &\approx \frac{i \sqrt{2} \sqrt{t - t_0}}{\sqrt{|(d^2 t/dp^2)(p_0)|}} [1 - ia_c (t - t_0)^{1/2}] \\ a_c &= \frac{\sqrt{2}}{6} \frac{(d^3 t/dp^3)(p_0)}{[(d^2 t/dp^2)(p_0)]^{3/2}}. \end{aligned} \quad (19)$$

Using this approximate contour, we may evaluate $[\operatorname{Re} R_n(t)]$ for several values of t and then use interpolation to find $[\operatorname{Re} R_n(t)]$ for other values of t . We then have

$$\psi \approx \sqrt{p_0/r} \frac{1}{\pi \eta_1(p_0)} \operatorname{Re} [R_n(t)] T(p_0) \left[\frac{d^2 t}{dp^2} (p_0) \right]^{-1/2} (t - t_0)^{-1/2}, \quad t > t_0. \quad (20)$$

We now have a complete time-domain description of ψ , which may be convolved with $1/\sqrt{t}$ and source terms using fast Fourier transform techniques.

It should be noted that the primary limiting factor to the validity of the modified first-motion approximations is the approximate contour (19). Where the reflected portion of the generalized ray is unimportant or if the contour has relatively little structure, the approximations will remain valid. Where the contour bends over quickly or has significant structure, as in tunnelling problems, or where exact determination of the contour is important, as in the treatment of surface waves, a better approximation of the contour must be employed.

Tests of the modified first-motion approximation

It has become almost traditional (Helmberger 1973; Chapman 1974) to test generalized ray-theory programs by attempting to compute the step-function response for a homogeneous

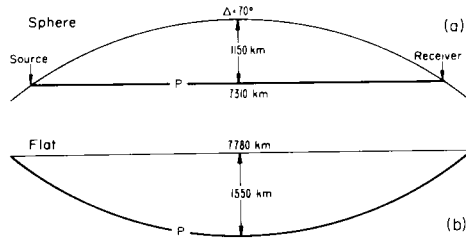


Figure 2. The earth-flattening approximation used for the test problem of a point source in a homogeneous whole-space.

fluid whole-space using an earth-flattening transformation. We begin with a homogeneous fluid whole-space, with a wave velocity of 6 km/s. On this space, we impose a spherical coordinate system. We choose our source and receiver to lie at a distance of 6371 km from the origin, separated by an angular distance of 70° . The sphere is divided into 25 km thick spherical layers, and the earth-flattening approximation is applied, giving a layered, flat, equivalent model. This process is illustrated in Fig. 2. The response for this model is then computed using only first-order reflections.

The homogeneous whole-space problem is an extremely good test of a generalized ray method, since the final response is a rather delicate superposition of a large number of first-order generalized rays. These include pre-critical reflections, critical reflections and post-critical refractions.

HOMOGENEOUS SPHERE $\Delta = 70^\circ$ $T_h = 25$ km

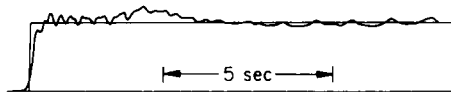


Figure 3. Comparison of the exact response for a point source in a homogeneous fluid and the MFM response for the equivalent earth-flattened model using only first reflections.

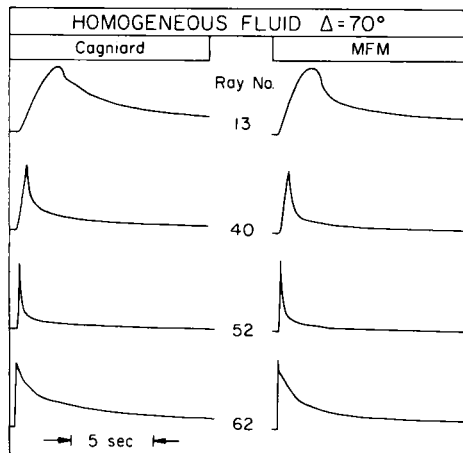


Figure 4. Comparison of MFM and full Cagniard for representative generalized rays from the earth-flattened homogeneous fluid problem. Ray number refers to the layer from which the generalized ray was reflected. Layer thickness is 25 km before earth flattening is applied. Corresponding MFM and Cagniard rays are to the same scale.

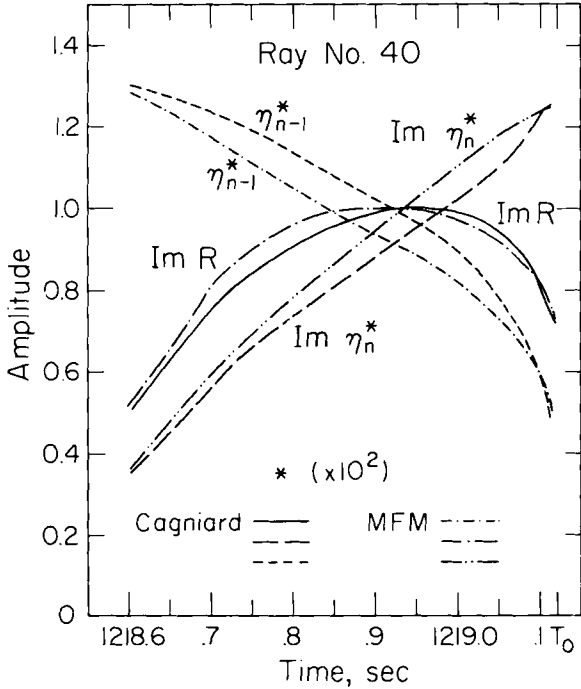


Figure 5. Comparison of several quantities critical to head-wave portion of Ray 40 for MFM and full Cagniard.

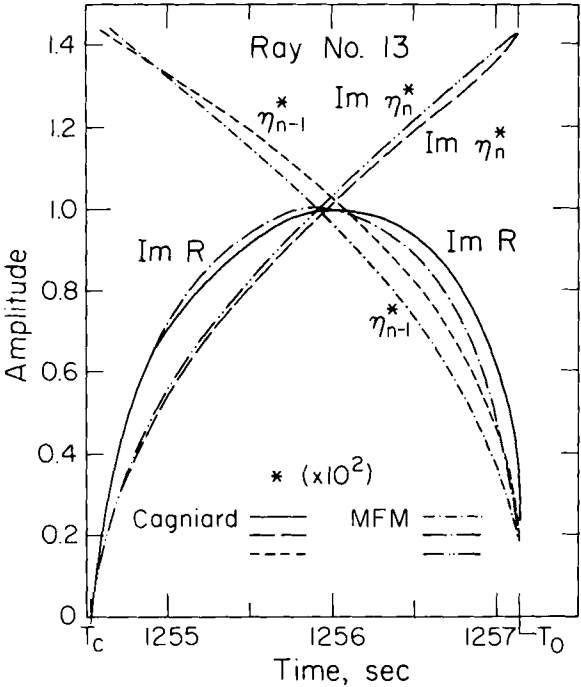


Figure 6. Comparison of several quantities critical to head-wave portion of Ray 13 for MFM and full Cagniard.

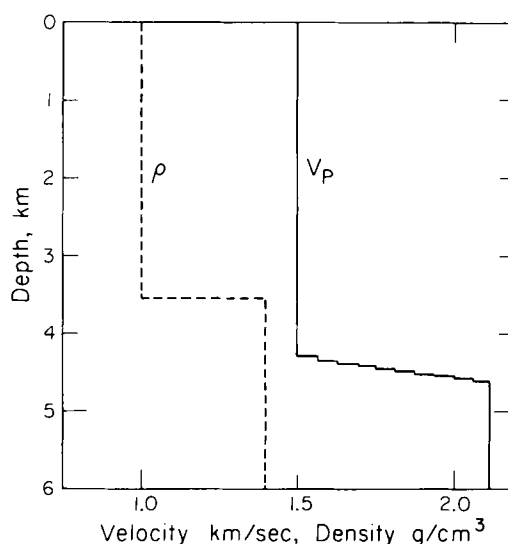


Figure 7. Velocity and density model for a simplified oceanic sub-bottom.

A comparison of the MFM solutions and the exact solution are given in Fig. 3. As may be seen, excellent agreement is obtained. The 'graininess' of the MFM solution is an artifact of the layering approximation, not of the MFM method itself, since a similar effect occurs for the full Cagniard-de Hoop method.

It is instructive at this point, to examine the ray response for several representative generalized rays from the whole-space problem. Fig. 4 presents a comparison of four such rays computed using MFM with the same rays computed using the full Cagniard-de Hoop method. The ray number identifying each ray is the number of the layer, from the top of the model, in which the reflection occurred. Ray 13 represents a well developed refraction, ray 40 represents a case where the refraction and critical reflection strongly interact, ray 52 represents a case in which $t_0 - t_c$ is comparable to the time spacing used to compute the ray and ray 62 represents a pre-critical reflection. In all cases, good agreement is obtained between the two methods.

Further insight into the operation of MFM may be gained by examining in detail the approximations for η_n , η_{n-1} and $\text{Im}(R_n)$ used in computing rays 40 and 13. Comparisons of the approximate and actual values of these quantities is given in Fig. 5 and 6. As may be seen, all quantities exhibit considerable structure not accounted for by standard first-motion approximations. In particular, the nearly linear behaviour of η_n near p_0 and the non-constant behaviour of η_{n-1} are not predicted by the standard first-motion approximations. However, using MFM good agreement is obtained.

Further comparisons of MFM and Cagniard-de Hoop have been made for the model shown in Fig. 7. This model may be viewed as presenting a somewhat simplified oceanic sub-bottom. The size of the density contrast was chosen so that in the long-period limit the amplitude of the reflections from the velocity gradient and from the density contrast will be equal for a source to receiver distance of 3 km.

Step-function responses were obtained using both Cagniard-de Hoop and MFM for a profile of eight distances which cover the development of the triplication. Synthetic seismograms were generated by convolving step responses with a system function previously used by Helmberger (1976) in oceanic studies. This function contains instrument and filter

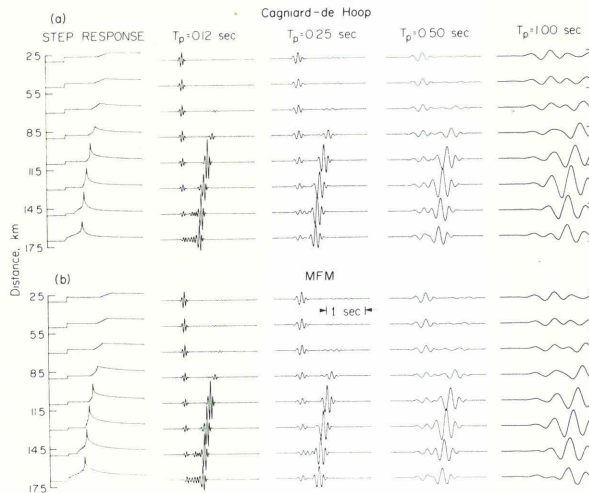


Figure 8. Comparison of synthetic seismograms generated using Cagniard-de Hoop (a) and MFM (b). Synthetics were produced using both methods for ranges of 3, 5, 7, 9, 11, 13, 15 and 17 km and for system functions with peak periods T_p of 0.12, 0.25, 0.5 and 1 s. The same scale is used in all synthetics in this figure so that amplitudes are directly comparable.

functions, as well as the source-time function. In order to study frequency dependent effects and thus investigate the behaviour of MFM over a relatively large frequency range, a number of system functions were derived from the original system function by either compression or expansion of the time axis. In this manner, system functions with peaks at 1, 0.5, 0.25 and 0.12 s periods were obtained.

Results of synthetic seismograms calculations for this model are shown in Fig. 8. The same scale is used in the profiles generated using Cagniard and MFM. Hence, amplitudes in Figs 8(a) and (b) are directly comparable. Comparisons of corresponding synthetic seismograms for the two methods used in general show excellent agreement.

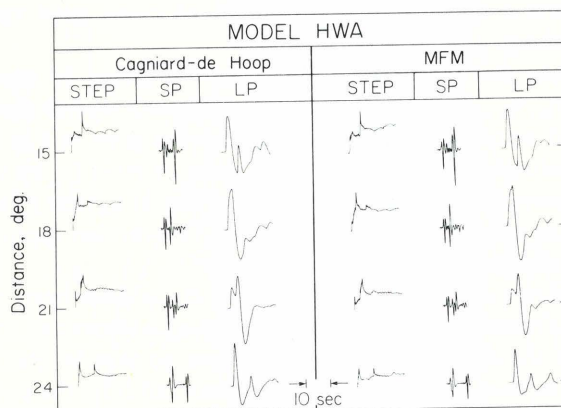


Figure 9. Comparison of synthetic seismograms for upper-mantle model HWA. Synthetics were produced for ranges of 15, 18, 21 and 24°. Step function and short and long-period WWSSN seismograms are shown. Short and long-period seismograms assume a delta function point source and a Futterman Q operator with $T/Q = 1$ s. Instrumental gain has been scaled for ease of presentation, but scale remains the same throughout the figure so that amplitudes may be directly compared.

The first arrival for all distances less than 17 km is the reflection from the density contrast. Amplitude of this reflection is determined by geometric spreading only and is otherwise independent of ray parameter. The reflection from the velocity gradient is a long-period phenomenon for small source to receiver distances, with short periods becoming increasingly evident for distances where the critical angle is approached. Once the critical angle is reached, a head wave develops in the velocity gradient. At distances of 15 and 17 km, this head wave has become well developed. The frequency-dependence of the reflection is readily apparent from comparisons of the 0.12 and 1 s system-function profiles.

An additional comparison has been made for an upper-mantle model, HWA of Wiggins & Helmberger (1973). Results of this comparison for a profile of four representative ranges are shown in Fig. 9. The step-function response, as well as seismograms including a Futterman (1962) Q operator with T/Q of 1 s for both short and long period WWNSS instruments have been computed. Good agreement between the Cagniard-de Hoop and MFM methods has been obtained in all cases. The MFM method however, required approximately $1/10$ the computer time of the Cagniard-de Hoop method.

Of particular interest is the good agreement obtained at 15° , since at this range there is significant energy arriving from both above and below the low-velocity zone. This indicates that MFM may well be useful in certain types of diffraction problems.

Conclusion

A series of modifications to the Cagniard-de Hoop first-motion approximations have been developed. These approximations provide explicit time-domain expressions for quantities used in calculating generalized rays, resulting in a significant saving in computer time. Tests performed for a homogeneous earth, for an oceanic sub-bottom triplication and for an upper-mantle triplication indicate that MFM will be useful for the calculation of synthetic seismograms in a wide variety of geophysically interesting problems.

Acknowledgments

The authors would like to thank L. J. Burdick for his assistance in comparison of the two methods used. This research was supported by the Office of Naval Research under Contract NR 083-399.

References

- Chapman, C. H., 1974. Generalized ray theory for an inhomogeneous medium, *Geophys. J. R. astr. Soc.*, **36**, 673–704.
- Chapman, C. H., 1976. Exact and approximate generalized ray theory in vertically inhomogeneous media, *Geophys. J. R. astr. Soc.*, **46**, 201–234.
- de Hoop, A. T., 1960. A modification of Cagniard's method for solving seismic pulse problem, *Appl. Sci. Res. B.*, **8**, 349–356.
- Futterman, W. I., 1962. Dispersive body waves, *J. geophys. Res.*, **67**, 5279–5291.
- Fuchs, K. & Muller, G., 1971. Computation of synthetic seismograms with the reflectivity method and comparison with observations, *Geophys. J. R. astr. Soc.*, **23**, 417–433.
- Gilbert, F. & Knopoff, L., 1961. The directivity problem for a buried line source, *Geophys.*, **26**, 626–634.
- Helmberger, D. V., 1968. The crust mantle transition in the Bering Sea, *Bull. seism. Soc. Am.*, **58**, 179–214.

- Helmberger, D. V., 1973. Numerical seismograms of long period body waves from seventeen to forty degrees, *Bull. seism. Soc. Am.*, **63**, 633–646.
- Helmberger, D. V., 1976. Fine structure of an Aleutian crustal section, *Geophys. J. R. astr. Soc.*, **48**, 81–90.
- Wiggins, R. A. & Helmberger, D. V., 1973. Upper mantle structure of the western United States, *J. geophys. Res.*, **78**, 1870–1880.
- Wiggins, R. A., 1976. Body-wave amplitude calculations – II, *Geophys. J. R. astr. Soc.*, **46**, 1–10.